Towards H2 production from water and ethanol interactions on hydrated TiO2(101): Insights from ReaxFF molecular dynamics

Hicham Jabraoui, Mehdi Djafari Rouhani, Carole Rossi, Alain Esteve

Highlights

Towards H_2 Production from Water and Ethanol Interactions on Hydrated TiO_2(101): Insights from ReaxFF Molecular Dynamics

Hicham Jabraoui, Mehdi Djafari Rouhani, Carole Rossi, Alain Esteve

- Exploring liquid ethanol/water interaction with hydrated-TiO_2(101) using ReaxFF molecular dynamics.
- Ethanol dissociation lowers TiO_2 hydration and hydrogen mobility through permanent bonding of ethoxy radicals on Ti surface sites.
- Water dominates the surface interactions when mixed with ethanol, maintaining a high level of surface hydration, i.e.,lowering ethoxy fixation.
- Mechanisms of surface hydration (i.e., generation of surface hydroxyls) via water or ethanol molecules all show activation barrier inferior to 0.5 eV.
- Calculation of the formation of H_2, while unlikely energetically, still shows the prevalence of catalytic (molecule/surface) rather than purely surfacic mechanisms.

Towards H_2 Production from Water and Ethanol Interactions on Hydrated TiO_2(101): Insights from ReaxFF Molecular Dynamics

Hicham Jabraoui[a,*], Mehdi Djafari Rouhani[a], Carole Rossi[a], Alain Esteve[a,**]

[a] *LAAS-CNRS University of Toulouse 31077 Toulouse France*

Abstract

ReaxFF molecular dynamics is employed to investigate interactions between water, ethanol, their mixture, and hydrated TiO_2(101) surfaces. Water maintains hydration, while exchanging both hydrogen and oxygen atoms with the surface. Ethanol dissociates, leading to the formation of ethoxy radicals (CH_3CH_2O) permanently attached to the surface, water molecules, and acetic acid (CH_3CO_2) species. Ethoxy reduces the number of hydroxyl groups and hinders hydrogen migration across the surface. The mixture of water, ethanol, and TiO_2(101) results in a reduction of ethoxy coverage, inhibits CH_3CO_2 formation, and increases hydroxyl coverage, indicating the dominant role of water. Potential of mean force analysis shows that hydroxyl formation follows exothermic paths, with activation energy lower than 0.45 eV. A narrower pathway for ethanol access to its adsorbed site is a key factor in the dominance of water. The formation of H_2 molecules exhibits a prohibitive energy barrier (> 4 eV), suggesting that catalytic pathways, rather than purely surface reactions, could be favored.

Keywords: Reactive force field molecular dynamics, Potential of Mean Force (PMF) analysis, water-ethanol-TiO_2 interface, hydrogen production, hydrated-TiO_2

*Corresponding author

**Corresponding author

Email addresses: hicham.jabraoui@gmail.com (Hicham Jabraoui), aesteve@laas.fr (Alain Esteve)

1. INTRODUCTION

The increasing global demand for sustainable energy sources has prompted an Highlights1 Towards H2 Production from Water and Ethanol Interactions on2 Hydrated TiO2(101): Insights from ReaxFF Molecular Dynamics3 Hicham Jabraoui, Mehdi Djafari Rouhani, Carole Rossi, Alain Esteve4 • Exploring liquid ethanol/water interaction with hydrated-TiO2(101)5 using ReaxFF molecular dynamics.6 • Ethanol dissociation lowers TiO2 hydration and hydrogen mobility through7 permanent bonding of ethoxy radicals on Ti surface sites.8 • Water dominates the surface interactions when mixed with ethanol,9 maintaining a high level of surface hydration, i.e.,lowering ethoxy fixa-10 tion.11 • Mechanisms of surface hydration (i.e., generation of surface hydroxyls)12 via water or ethanol molecules all show activation barrier inferior to13 0.5 eV.14 • Calculation of the formation of H2, while unlikely energetically, still15 shows the prevalence of catalytic (molecule/surface) rather than purely16 surfacic mechanisms.17 Towards H2 Production from Water and Ethanol18 Interactions on Hydrated TiO2(101): Insights from19 ReaxFF Molecular Dynamics20 Hicham Jabraouia,, Mehdi Djafari Rouhania, Carole Rossia, Alain Estevea, 21 aLAAS-CNRS University of Toulouse 31077 Toulouse France Abstract22 ReaxFF molecular dynamics is employed to investigate interactions between23 water, ethanol, their mixture, and hydrated TiO2(101) surfaces. Water main-24 tains hydration, while exchanging both hydrogen and oxygen atoms with25 the surface. Ethanol dissociates, leading to the formation of ethoxy radi-26 cals (CH3CH2O) permanently attached to the surface, water molecules, and27 acetic acid (CH3CO2) species. Ethoxy reduces the number of hydroxyl groups28 and hinders hydrogen migration across the surface. The mixture of water,29 ethanol, and TiO2(101) results in a reduction of ethoxy coverage, inhibits30 CH3CO2 formation, and increases hydroxyl coverage, indicating the domi-31 nant role of water. Potential of mean force analysis shows that hydroxyl32 formation follows exothermic paths, with activation energy lower than 0.4533 eV. A narrower pathway for ethanol access to its adsorbed site is a key factor34 in the dominance of water. The formation of H2 molecules exhibits a pro-35 hibitive energy barrier (> 4 eV), suggesting that catalytic pathways, rather36 than purely surface reactions, could be favored.37 Keywords: Reactive force field molecular dynamics, Potential of Mean38 Force (PMF) analysis, water-ethanol-TiO2 interface, hydrogen production,39 hydrated-TiO240 Corresponding author Corresponding author Email addresses: hicham.jabraoui@gmail.com (Hicham Jabraoui),

aesteve@laas.fr (Alain Esteve) Preprint submitted to Applied Surface Science 1. INTRODUCTION41 The increasing global demand for sustainable energy sources has prompted42 an urgent search for alternative and eco-friendly solutions. Molecular hydro-43 gen (H2) has emerged as a promising candidate, offering a clean and highly44 efficient energy prospect. However, the natural occurrence of hydrogen atoms45 being typically bound to other elements renders the direct sourcing of molec-46 ular hydrogen impractical. Consequently, intensive exploration of technolog-47 ical pathways to produce hydrogen has been ongoing for decades [? ? ?48 ? ? ?]. One such historical path is to make use of photocatalytic sur-49 faces to achieve the photoreduction of water (the so-called water splitting);50 in this framework, titanium dioxide (TiO2), because of remarkable photo-51 catalytic capabilities, made early demonstrations of water splitting-induced52 hydrogen production [? ? ? ?]. Since then, TiO2(101) has imposed it-53 self as the most studied model surface to investigate the fundamentals of54 water splitting chemistry and electrochemistry both theoretically [?] and55 experimentally [? ?]—i.e., the role of surface chemistry, crystallinity, grain56 boundaries and orientation, doping, defects, charges (lifetime, localization,57 and transport). Among the various phases of TiO2, anatase stands out for58 its superior efficiency in separating electrons and holes, partly facilitated by59 its larger bandgap [?]. While the exact reasons for this superior perfor-60 mance are still under debate due to the multiplicity of factors influencing the61 photocatalytic process, anatase represents the best model system to date, for62 which the literature is much more abundant.63 Theoretically, atomistic simulation studies have been limited to rather64 small systems, essentially treating single molecule interactions on the TiO265 surface, such as water [? ? ? ? ? ? ? ?], or ethanol [?]. Similarly, other66 surfaces of technological interest have been investigated, such as alumina [?67] and silica [?]. In this framework, the liquid-solid interface has been poorly68 studied from a physico-chemical standpoint.69 Alcohol, such as ethanol (via the photodehydrogenation of ethanol to form70 molecular hydrogen and acetaldehyde [? ?]), and water can be considered71 as direct chemical agents for hydrogen production. Ethanol is supposed to be72 thermodynamically more efficient (G0 = +237 kJ·mol-1 for water oxidation73 versus G0 = +41.5 kJ·mol-1 for ethanol oxidation), reducing the energy74 input required [? ?]. Note that ethanol is also commonly used as an additive75 to water solvent, acting as a sacrificial agent (hole scavenger), allowing for76 charge separation and lowering the recombination rate, leading to better77 2 production performances.

Finally, in the photocatalytic process, ethanol can78 prevent the generation of O2 species by producing carboxylic groups. All79 these characteristics make it difficult to predict which process will finally80 dominate when mixing water and ethanol, as the collective arrangement of81 these molecules in contact with the surface is not known.82 Importantly, along the same line, the surface hydration level in contact83 with different liquid mediums is one key factor of the photocatalytic response84 and its durability (stability of the surface chemistry, i.e., hydration stability)85 [?]. Despite all, this aspect has never been addressed so far.86 This work employs ReaxFF molecular dynamics simulations to investigate87 and quantify the interaction of different liquid environments, i.e. pure water88 and ethanol phases before studying a mixing of them, on a realistic thus89 hydrated TiO2 surface. This allows focusing on the persistence of hydration,90 and specific chemical mechanisms involved in this type of configuration. The91 choice of ReaxFF MD simulations is grounded in its robustness to investigate92 reactivity at the interface between water, alcohol, and mineral materials,93 including TiO2 [? ? ?]. The study provides new insights into how water94 and ethanol react to eventually decompose in contact with the hydrated TiO295 surface, influencing the generation of radicals, including hydroxyl groups.96 Additionally, by employing the Potential of Mean Field (PMF) technique,97 we investigate in greater detail the energetics of hydration pathways and98 discuss tentative scenarios for producing hydrogen without consideration of99 external excitation, photonic, or electronic.100 2. COMPUTATIONAL DETAILS101 In this study, we conducted molecular dynamics (MD) simulations with102 periodic boundary conditions using the LAMMPS package [?]. The temper-103 ature within the NVT ensemble was controlled using the Nosé-Hoover ther-104 mostat. We employed a reactive force field based on the ReaxFF framework105 to model the interatomic interactions at the interfaces of TiO2(101) with liq-106 uid ethanol, water, and a mixture of both species. The force field parameters107 were defined according to previous work by Kim and van Duin [?]. The108 TiO2 supercell was generated with the anatase crystal structure, featuring a109 tetragonal unit cell with lattice parameters a = b = 3.78 Å, c = 9.62 Å, and110 = = = 90◦. The space group assigned to the supercell was I41/amd111 [?]. To create the (101) surface, we followed a specific procedure resulting112 in face-to-face (101) planes, each with dimensions of 31.40 Å × 38.03 Å and113 3 urgent search for alternative and eco-friendly solutions. Molecular hydrogen (H_2) has emerged as a promising candidate, offering a clean and highly efficient

energy prospect. However, the natural occurrence of hydrogen atoms being typically bound to other elements renders the direct sourcing of molecular hydrogen impractical. Consequently, intensive exploration of technological pathways to produce hydrogen has been ongoing for decades [1, 2, 3, 4, 5, 6]. One such historical path is to make use of photocatalytic surfaces to achieve the photoreduction of water (the so-called water splitting); in this framework, titanium dioxide (TiO_2), because of remarkable photocatalytic capabilities, made early demonstrations of water splitting-induced hydrogen production [2, 7, 8, 9]. Since then, TiO_2(101) has imposed itself as the most studied model surface to investigate the fundamentals of water splitting chemistry and electrochemistry both theoretically [8] and experimentally [10, 11]—i.e., the role of surface chemistry, crystallinity, grain boundaries and orientation, doping, defects, charges (lifetime, localization, and transport). Among the various phases of TiO_2, anatase stands out for its superior efficiency in separating electrons and holes, partly facilitated by its larger bandgap [12]. While the exact reasons for this superior performance are still under debate due to the multiplicity of factors influencing the photocatalytic process, anatase represents the best model system to date, for which the literature is much more abundant.

Theoretically, atomistic simulation studies have been limited to rather small systems, essentially treating single molecule interactions on the TiO_2 surface, such as water [7, 13, 8, 1, 2, 3, 4, 6], or ethanol [4]. Similarly, other surfaces of technological interest have been investigated, such as alumina [14] and silica [15]. In this framework, the liquid-solid interface has been poorly studied from a physico-chemical standpoint.

Alcohol, such as ethanol (via the photodehydrogenation of ethanol to form molecular hydrogen and acetaldehyde [16, 17]), and water can be considered as direct chemical agents for hydrogen production. Ethanol is supposed to be thermodynamically more efficient ($\Delta G^0 = +237$ kJ·mol^{-1} for water oxidation *versus* $\Delta G^0 = +41.5$ kJ·mol^{-1} for ethanol oxidation), reducing the energy input required [18, 19]. Note that ethanol is also commonly used as an additive to water solvent, acting as a sacrificial agent (hole scavenger), allowing for charge separation and lowering the recombination rate, leading to better production performances. Finally, in the photocatalytic process, ethanol can prevent the generation of O_2 species by producing carboxylic groups. All these characteristics make it difficult to predict which process will finally dominate when mixing water and ethanol, as the collective arrangement of these molecules in contact with the surface is not known.

Importantly, along the same line, the surface hydration level in contact with different liquid mediums is one key factor of the photocatalytic response and its durability (stability of the surface chemistry, i.e., hydration stability) [3]. Despite all, this aspect has never been addressed so far.

This work employs ReaxFF molecular dynamics simulations to investigate and quantify the interaction of different liquid environments, *i.e.* pure water and ethanol phases before studying a mixing of them, on a realistic thus hydrated TiO_2 surface. This allows focusing on the persistence of hydration, and specific chemical mechanisms involved in this type of configuration. The choice of ReaxFF MD simulations is grounded in its robustness to investigate reactivity at the interface between water, alcohol, and mineral materials, including TiO_2 [20, 7, 21]. The study provides new insights into how water and ethanol react to eventually decompose in contact with the hydrated TiO_2 surface, influencing the generation of radicals, including hydroxyl groups. Additionally, by employing the Potential of Mean Field (PMF) technique, we investigate in greater detail the energetics of hydration pathways and discuss tentative scenarios for producing hydrogen without consideration of external excitation, photonic, or electronic.

2. COMPUTATIONAL DETAILS

In this study, we conducted molecular dynamics (MD) simulations with periodic boundary conditions using the LAMMPS package [22]. The temperature within the NVT ensemble was controlled using the Nosé-Hoover thermostat. We employed a reactive force field based on the ReaxFF framework to model the interatomic interactions at the interfaces of TiO_2(101) with liquid ethanol, water, and a mixture of both species. The force field parameters were defined according to previous work by Kim and van Duin [23]. The TiO_2 supercell was generated with the anatase crystal structure, featuring a tetragonal unit cell with lattice parameters $a = b = 3.78$ Å, $c = 9.62$ Å, and $\alpha = \beta = \gamma = 90°$. The space group assigned to the supercell was $I4_1/amd$ [24]. To create the (101) surface, we followed a specific procedure resulting in face-to-face (101) planes, each with dimensions of 31.40 Å × 38.03 Å and a slab height of approximately 24 Å. Before surface formation, the bulk supercell underwent relaxation in the NVT ensemble for 0.1 nanoseconds (ns) using a time step of 1 femtosecond (fs). Subsequently, we constructed the final supercell as depicted in Figure 1, comprising two bulk cells separated by vacuum spaces of (45 and 26 Å). We ran the relaxation process in the NVT

ensemble at a temperature of 300 K for an additional 0.1 ns, with a time step of 1 fs. The overall TiO_2(101) region contained 1662 O atoms and 831 Ti atoms. The smaller vacuum space was designated to be filled with liquid phases. The face-to-face surfaces were chosen to increase the likelihood of significant events from a statistical standpoint (see Figure 1a). This structure also facilitated the breathing of the liquid phase during relaxation, preventing contamination from potential molecule evaporation or pressure effects. The choice of the (101) anatase plane to represent TiO_2 was based on its distinct chemical reactivity and adsorption characteristics towards water and other protonated molecules (e.g., ethanol, methanol). Additionally, TiO_2(101) is the most stable and predominant surface for nanocrystals, occupying over 94% of the total surface area [25].

With the goal of constructing hydrated TiO_2(101) surfaces, we introduced water molecules to protonate and hydroxylate surface sites on the two exposed surfaces. To achieve this, the system was relaxed at 300 K in the NVT ensemble, using a time step of 0.5 fs for a simulation period of 1 ns. The density of the water molecules placed in the vacuum was set to 1 g/cm^3. After the relaxation process, we removed water molecules that maintained their molecular form, while the dissociated water components were retained on the surfaces. These resulting functional groups enhanced the hydrogen bond networking with the outer surface, leading to a delicate network of interaction dynamics. It became evident that a smaller time step than 1 fs was necessary to accurately simulate the behavior of water and the hydrated system [20, 26, 27, 28], and notably the Grotthuss kind of mechanism [29]. Consequently, we successfully obtained two hydrated surfaces exposed to a vacuum environment (see Figure 1b).

To construct the liquid medium, we introduced 882 water molecules, as depicted in Figure 1c, along with 500 ethanol molecules with a density of 0.8 g/cm^3, as illustrated in Figure 1d. Additionally, we created a precise balanced mixture comprising 445 water molecules and 288 ethanol molecules (in a 1:1 volume ratio). In this mixture, the density of water was maintained at 1 g/cm^3, while ethanol had a density of 0.8 g/cm^3, as shown in Figure 1e. This arrangement was designed to occupy the vacuum space between the two hydrated surfaces. Subsequently, these liquid/surface interfaces underwent relaxation at 400 K in the NVT ensemble, using a time step of 0.5 fs over 6 ns.

To gain further insights into the energetics and reaction pathways of a selection of chemical reactions of interest, not necessarily occurring during

the elapsed simulations (such as molecular hydrogen production), we conducted Molecular Dynamics (MD) simulations employing the Potential of Mean Force (PMF) method [30]. Before commencing the PMF simulations, we ensured that the system attained thermodynamic equilibrium by allowing it to relax at room temperature. Subsequently, we applied a moving harmonic potential to control the system's behavior during the simulations in a desired way.

For these simulations, we utilized the steered molecular dynamics (SMD) algorithm, implemented within the LAMMPS software package [31, 32, 33, 34, 35]. In this framework, we applied a constant velocity along the negative direction to one of the atoms from ethanol or water molecules involved in the chemical reaction. This approach facilitated the formation of a bond between the selected hydrogen atom and a targeted atom present at the surface or in the solution. To achieve this, a spring constant (K) of $1{\times}10^4$ kcal/mol/Å was applied to steer the selected atoms towards each other. To ensure the reliability of our simulations, the pulling velocity was set to -0.00005 Å per femtosecond [36, 35]. This choice enabled a smooth and controlled approach of the target atom towards the surface, minimizing significant perturbations to the overall system, including the local environment in contact with the constrained atoms.

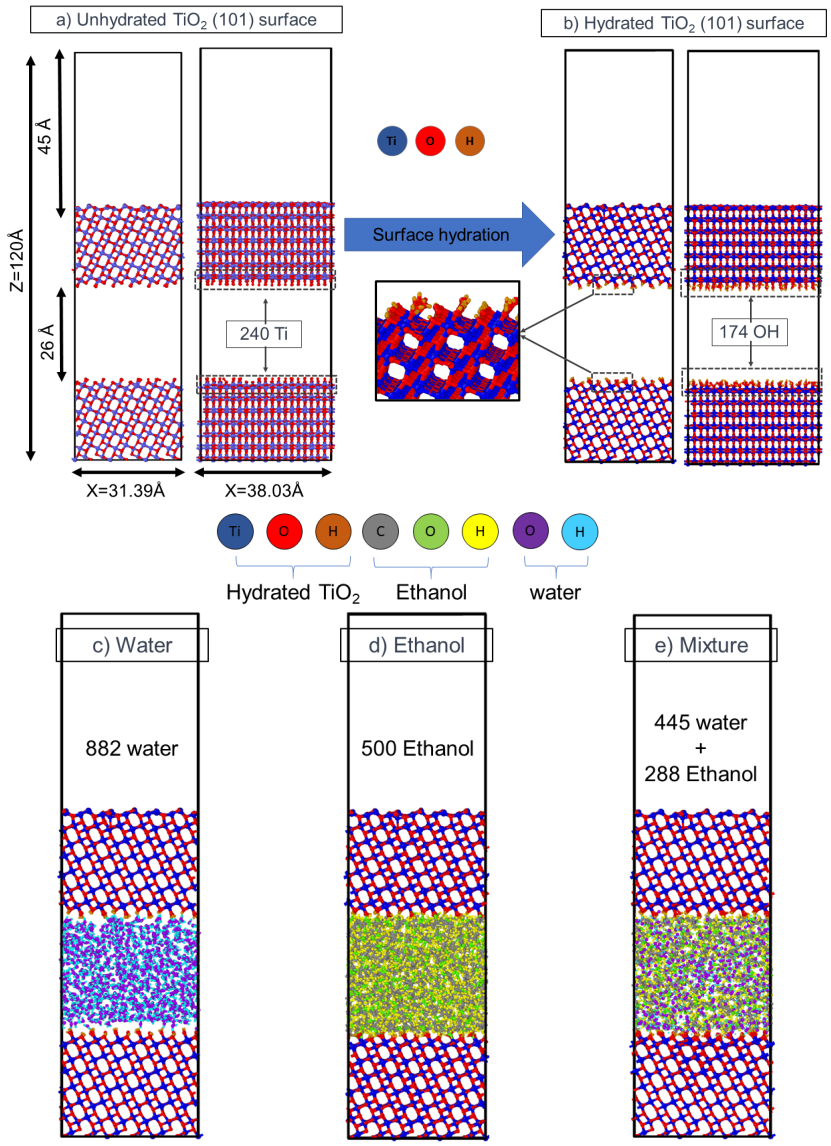

Figure 1: Side-view schematics of the initial atomic-scale model of the anatase $TiO_2(101)$ surface, depicting both the (a) unhydrated and (b) hydrated (101) surfaces. Side view schematics of the water-$TiO_2(101)$ interface (c), the ethanol-$TiO_2(101)$ interface (d), and the mixture of ethanol and water-TiO_2-(101) interface (e). The $TiO_2(101)$, water, and ethanol atoms are visually represented with red, blue, orange, green, grey, yellow, purple, and sky blue spheres, representing O_{TiO_2}, Ti, H_{TiO_2}, $O_{Ethanol}$, $C_{Ethanol}$, $H_{Ethanol}$, O_{H2O}, and H_{H2O} atoms, respectively.

3. RESULTS AND DISCUSSION

This section is divided into two main subsections. First, a statistical analysis of the interaction between hydrated TiO_2(101) and three liquid phases is presented: monomolecular liquids, *e.g.*, water and ethanol, serving as reference interfaces to further investigate the more complex interaction of a mixture of water and ethanol with hydrated titanium dioxide, see Figure 1(c-d) for initial interfaces and Figure SM1(a-c) for interfaces after MD run. Note that for quantifying the various radicals present on the three interfaces, we use the number of top surface Ti-sites (in direct contact with the liquid phases) as the reference, which amounts to 240 and remains unchanged during the annealing. From this reference, the percentage of each identified radical at the interface is calculated using the following equation:

$$\text{radical}(\%) = \text{Number of a radical} \times \left(\frac{100}{240}\right).$$

Subsequently, we proceed to a more detailed analysis of specific surface chemistries (pathways and energetics) using the PMF technique. Notably, we determine the OH formation pathways from the liquid phase which governs the hydration level of the surface. This method also allows investigating rare or even non-occurring events during the elapsed simulations.

3.1. Statistical Analysis of Interfacial Events

3.1.1. Interactions at the Water-TiO_2(101) Interface

In this subsection, all calculations are performed at 400 K. Figure 2 focuses on the water/surface protonic exchange. From Figure 2a, green curve, a nearly constant number of hydroxyl groups (OH) is observed throughout the entire 6 ns simulation, with an average number of about 188 OHs (78% coverage as referred to as the total number of Ti-adsorption sites), averaged over the last ns. Note that this results in a slight increase of the number of hydroxyl groups compared to the initial hydration procedure at 300 K. Despite this apparent global chemical stability of the hydrated surface, a closer examination of the interactions shows substantial chemical activity at the interface. A dynamic process of hydrogen exchange between water molecules and the hydrated TiO_2 surface is taking place. Indeed, a vast number of hydroxyl groups are generated from the decomposition of water molecules that stabilizes at about 173 OHs (72% coverage). Concomitantly, a number of hydrogen atoms initially associated with the hydrated TiO_2 are released

into the bulk water, which loss compensates the protonic gain due to protons released from dissociated water. *In fine*, almost all initial surface hydrogen atoms have been replaced by hydrogen emanating from the water medium (surface coverage of hydrogen illustrated by blue spheres in Figure 2c). From the simulation, the exchange is always local, either direct ($H_{TiO_2} \leftrightarrow H_{H_2O}$), or indirect, involving nearest neighbours and Grotthuss type of mechanisms. This overall exchange of hydrogen atoms between the surface and the liquid water results in an equilibrium state between the two phases where occurrence of the exchange mechanisms is still but rarely observed. In Figure 2b, the peak associated with the shortest surface OH bond length after reaching interface equilibrium, in the range 0.93-1.03 Å, considering oxygen and hydrogen species initially belonging to different medium (liquid or solid), demonstrates that hydrogen exchange has been operated. The $O_{TiO_2}-H_{H_2O}$ peak at around 1.8 Å is due to the hydrogen bonding of non-dissociated water molecules on surface adsorption sites. In a previous ReaxFF MD simulation investigation, Raju et al · [7] studied the adsorption and dissociation dynamics of water at 300 K on unhydrated TiO_2 surfaces. Specifically, they focused on anatase (101), (100), (112), (001), and rutile (110) surfaces, considering various water coverages. Their results unveiled a clear correlation between the extent of water dissociation on the various surfaces and the strength of hydrogen bonding between the adsorbed water molecules and those located outside the adsorbed layer. In a separate study by Huang *et al.* [13], molecular dynamics simulations using the ReaxFF force field were employed to hierarchize the reactivity in term of water dissociation on different TiO_2 surfaces [rutile (011) > monoclinic crystal (100) > anatase (001) > rutile (110)], with no observed water dissociation on the monoclinic crystal (001) surface. Additionally, their simulations highlight changes in water dissociation and TiO_2 surface chemistry, emphasizing the impact of new surface Ti–OH and O–H functional groups on the orientation of nearby water molecules.

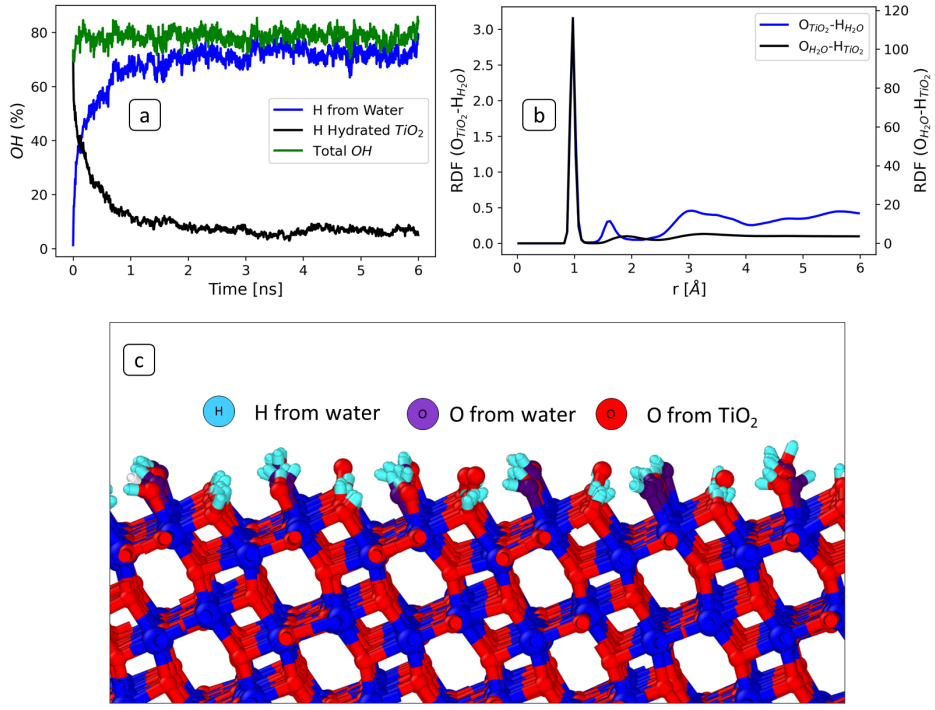

Figure 2: Water-hydrated $TiO_2(101)$ interface after 6 ns of annealing at 400 K: (a) Evolution of: the number of hydroxyl groups, number of surface hydrogen initially belonging to the water medium, and hydrogen released from the initial hydrated $TiO_2(101)$ into bulk water, (b) Radial distribution function (RDF) plots for H_{TiO2}-O_{H_2O} and H_{H_2O}-O_{TiO_2}, (c) Visualization of the $TiO_2(101)$ surface after 6 ns of annealing at 400K. Different colors are used to represent $O_{TiO_2(101)}$ (red), Ti (blue), O_{H_2O} (purple), and H_{H_2O} (sky blue) atoms. Note that no hydrogen atom from the initial bare hydrated surface is present after 6 ns, due to the exchange process with water. The number of H forming OH hydroxyl at the surface is calculated for the cutoff O−H= 1.2 Å.

Purple atoms representing oxygen atoms initially belonging to water molecules form more than half of the surface OH groups on the hydrated surface in Figure 2c. This already suggests that, beyond hydrogen exchange, oxygen exchange is also occurring, which is analyzed in greater detail in Figure 3. During the relaxation process, non-dissociated water molecules occupy binding sites on the hydrated $TiO_2(101)$ surface, establishing two types of bonding:

- Hydrogen bonding on the surface bridging ($H\text{——}O\text{——}H\cdots O_{TiO_2}$, see Figure 3c).

- A dative bond between a water oxygen atom and a top surface Ti atom (Figure 3d).

From these adsorption sites, some O_{H_2O} atoms involved in these interactions integrate into the surface, mostly as OH groups (Figure 2c, and Figure 3a, blue curve). This reaches an average value of 44 within the last nanosecond (18% coverage), while others remain in their molecular, non-dissociative configuration. Concurrently, but to a lesser extent, some oxygen atoms originally belonging to the hydrated $TiO_2(101)$ surface are released into the bulk water. These detached oxygen atoms combine to form new water molecules in the water phase, with the average number reaching 18 within the last nanosecond (about 6% coverage loss). Both the surface-inserted O_{H_2O} atoms and the number of water-released O_{Ti_2O} atoms increase during the annealing period. However, the increase in the number of oxygen atoms binding to the surface is more significant, indicating a net gain of oxygen atoms on the $TiO_2(101)$ surface after the entire relaxation process (Figure 3a). Examination of the radial distances between Ti atoms with O_{H_2O} and O_{Ti_2O} is another illustration of the adsorption and exchange processes taking place at the interface.

In summary, two mechanisms contribute to the enrichment of the hydration of the $TiO_2(101)$ surface through the dissociation of water molecules. The first involves the adsorption of water via one of its hydrogens on a free oxygen site, resulting in the formation of the surface structure ($H-\!\!-O-\!\!-H\cdots O_{TiO_2}$). Thus, an adsorbed proton from water can bind to the free oxygen site to form OH at the surface, instead of merely undergoing adsorption if the oxygen site carries an excess of negative charge, acting as a Lewis acid site [37, 38, 39]. The second mechanism occurs after water adsorption via its oxygen onto the exposed Ti-adsorption sites, which can lead to the formation of OH^- hydroxyl groups after the generation of a proton. In this case, the proton is only generated if the Ti-adsorption site exhibits an excess of positive charge, necessitating the presence of OH^-.

In this context, we compare the charge distribution of Ti in the five layers of the $TiO_2(101)$ surface exposed to water molecules between the first frame of annealing and the last frame, after 6 ns of annealing. Figure SM2 shows Ti net charges after the first frame of annealing and a given frame after 6 ns of annealing. Some surface atoms of the first layer exhibit a gain of charge, indicating their need for a positive charge to reach equilibrium (0.04 e gain), while some atoms in the subsurface show a loss of positive

charge (about 0.03 e loss), indicating their need for a negative charge to reach equilibrium. Here, Ti atoms from the surface present O non-bridging configuration, needing an H^+ as a positive charge, while subsurface Ti will needs an undercoordination value, which requires OH^- as a negative charge. After the dissociation of this adsorbed water, the liberated proton can either return to the solution, participating in the water network or recombine with a leaving surface hydroxyl. Note that water adsorption cannot be considered isolated, as a collective network of hydrogen atoms is constituted within the interface involving both water molecules and surface atoms [37]. Tilocca and Selloni [40] used DFT-GGA and DFT+U simulations to investigate the effect of a reducing subsurface Ti interstitial defect on the structure and reactivity of thin water layers on reduced TiO_2(101) surfaces, finding that the defect enhances the surface reactivity and alters the structure of the water layers. More recent investigations detailed the energetics of bonding and dissociation behavior of a single water molecule on various subsurface defects pointing to the influence of oxygen vacancy (shown to be unstable upon water dissociation) and Ti interstitial notably [2, 41], that should be extended and compared to similar surface configurations but exposed to water.

The formation of H——O bridges and non-bridging oxygen species indicates the creation of surface complexes that stabilize water molecules on the surface. Interaction of water with the surface via its hydrogen results in the slight elongation of associated surface Ti-O bonds at about 1.9 Å, as shown in Figure 3b and Figure 3c. Meanwhile, there is another type of oxygen from water close to the surface, maintaining its molecular form with a distance of 2.33 Å, as also illustrated in Figure 3d, representing a non-dissociative adsorption of water *via* its oxygen onto the exposed Ti of the surface. Note that the presence of additional oxygen atoms on the surface was shown to influence the material's reactivity, affecting its performance as a catalyst in water-splitting reactions or pollutant degradation [42].

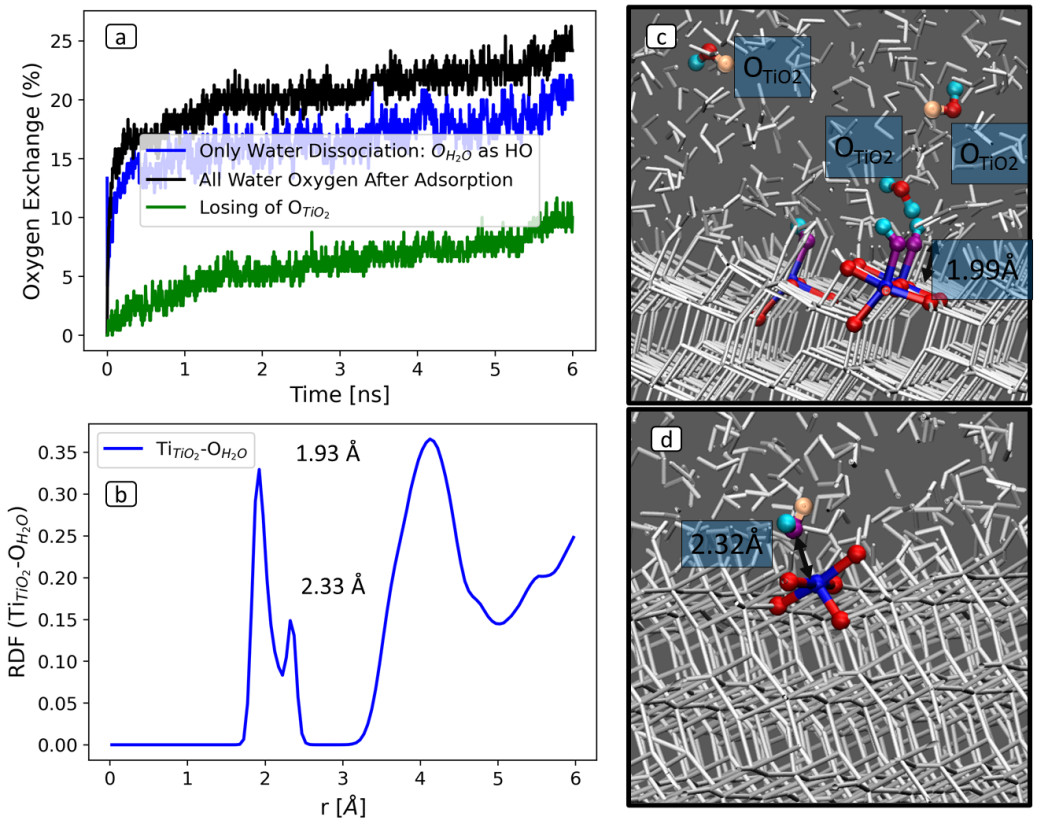

Figure 3: Water-hydrated $TiO_2(101)$ interface after 6 ns of annealing at 400 K: (a) Evolution of the insertion of O_{H_2O}, following water dissociation that turn into hydrated $TiO_2(101)$ surfaces (blue curve), all oxygen adsorbed (dissociative and non-dissociative adsorption) into hydrated $TiO_2(101)$ surfaces (black curve), and the release of O_{Ti_2O} with the green curve, (b) Comparing the Radial Distribution Function (RDF) for $Ti_{TiO_2(101)}$-O_{H_2O} and Ti_{TiO_2}-O_{TiO_2}, (c) the hydration of sites in the hydrated $TiO_2(101)$ surface resulting from the dissociation of water molecules, (d) the adsorption configuration of water onto the hydrated $TiO_2(101)$ surface, where different colors are used to represent O_{TiO_2} (red), Ti (blue), H_{TiO_2} (orange), O_{H_2O} (purple), and H_{H_2O} (sky blue) atoms.

3.1.2. Interactions at the Ethanol-TiO_2(101) Interface

Under the same conditions as before, *i.e.*, 6 ns of annealing at 400 K, the hydrated $TiO_2(101)$ surface is now exposed to pure ethanol. In contrast to water exposure, Figure 4a shows a slight decrease in the total number of OH groups present on the surface, down to 63% coverage, pointing to a lowering of the hydration level. A visual representation of the surface hydration after annealing can be seen in Figure 4c, where ethanol has been removed from

the structure. The figure indicates that some ethanol has dissociated, leaving ethoxy radicals (CH_3CH_2O) bonded to surface Ti atoms with a coverage of about 13.5% (about 33 ethoxy). Note that, in contrast to water exposure, a great percentage of hydrogen atoms participating to the initial surface hydration are still present on the surface (orange spheres), showing that the exchange process is less efficient in this case, limited to the number of ethanol that have dissociated. In another word, no direct exchange is taking place between ethanol and the surface. Rather, exchange is taking place via hydrogen from dissociated ethanol that are present on the surface, notably on bridging oxygen sites. RDF is another way to picture the exchange process. The Figure 4b) shows the RDF of H and O species belonging to different medium (water/ or surface, see .

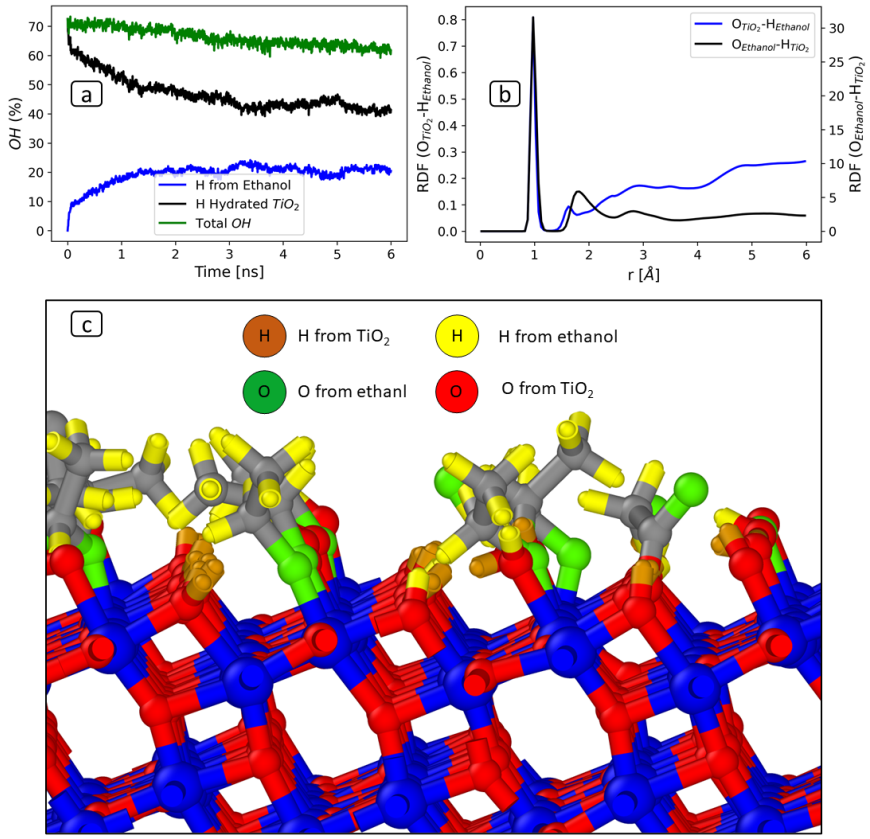

Figure 4: Ethanol-hydrated TiO_2 (101) interface after 6 ns of annealing at 400 K. (a) Time evolution of: the total number of hydroxyl groups, the number of surface hydrogen initially belonging to ethanol, and hydrogen released from the initially hydrated TiO_2 (101), (b) Radial distribution function (RDF) plots for H_{TiO2}-O_{H2O} and H_{H2O}-O_{TiO2}, (c) Visualization of the hydration structure after 6 ns of annealing at 400 K: O_{TiO_2} (red), Ti (blue), H_{TiO_2} (orange), $C_{Ethanol}$ (gray) atoms, $H_{Ethanol}$ (yellow) atoms, and $O_{Ethanol}$ (green) atoms. The number of H atoms forming OH hydroxyl at the surface is calculated for the cutoff O−H= 1.2 Å.

Importantly, under ethanol exposure, the formation of water molecules is observed, pointing to the nature of ethanol dissociation chemistry at the surface. As the simulation progresses, we notice a steady increase in the number of water molecules, eventually reaching a count of 34 water molecules (representing 14% of coverage). From Figures 5a and c, the number of water molecules being generated coincides with the dissociative adsorption of ethanol on surface OHs. To this respect the water molecules being created

are composed of a hydrogen atom originating from the ethanol OH termination bonded to a surface hydroxyl (Figures 5a blue and black curves). Figures 5c confirms that each water molecule that is created is associated with a dissociative adsorption of ethanol. Analyzing the radial distribution function in Figure 5b, we observe a Ti——O peak signature at 1.9 Å that is slightly shifted compared to initial Ti——OH, corresponding to ethoxy (CH_3CH_2O) radical bonded to surface Ti *via* its oxygen. The additional peak at 2.3 Å is another indirect signature of ethanol reaction, as it corresponds to the adsorption of the newly created water molecule on top of a neigbouring surface Ti atom, as illustrated in Figures 5d. The resulting water is confined nearby the TiO_2(101) surface, forming a layer of mixed water and CH_3CH_2O molecules as new derivative of ethanol species. The observed time-dependent formation of CH_3CH_2O radical molecules exclusively occurs on the Ti-adsorption site through oxygen. From the crowding of ethoxy radicals seen in Figure 4c, despite the non saturation of the various chemical processes being present, a steric hindrance is expected to play an essential role in limiting the kinetics and population of grafted ethoxy's. One main conclusion that may be drawn at this stage is that, in contrast to the propensity of water to keep TiO_2(101) fully hydrated, ethanol is shown to dehydrate the surface, by replacing surface hydroxyl species by ethoxy radicals, with potential shadowing of other surface regions due to steric hindrance. Further examining surface configurations, non-dissociative ethanol adsorption is quasi exclusively observed in a configuration where the interaction is driven by the ethanol CH subunit. A combination of Density Functional Theory (DFT) and Scanning Tunneling Microscopy (STM) images distinguished two types of surface adsorbates upon ethanol exposure [43]. These adsorbates can be attributed to the molecular and dissociative (in agreement with our calculated configurations) modes of ethanol interacting with the surface. Furthermore, DFT calculations demonstrated that the dissociative adsorption of ethanol was the most stable configuration, with an adsorption energy of -0.89 eV, compared to -0.72 eV for the non-dissociative adsorption [44]. This value is slightly higher than the adsorption energy of water on TiO_2(101), for which the calculated adsorption energy per molecule is 0.67 eV [45]. Another DFT investigation explored the adsorption and dissociation of ethanol on different surfaces of anatase TiO_2 [46]. Among these surfaces, the TiO_2(101) surface exhibited the most favorable product for the initial dissociation step of ethanol, confirming the ethoxy formation. The energy barrier for this step was calculated to be 0.96 eV [46]. In addition to these prevailing events, we

also observed a few instances (3 occurrences, 1.5 % equivalent coverage) of carboxylic acid radicals, namely acetic acid CH_3CO_2 formation, as commonly envisaged in the photocatalysis literature. These compounds adhere closely to the surface *via* oxygen at Ti-adsorption sites, maintaining a separation distance of about 1.4 Å, as shown in Figure 6. Interestingly, the process of converting ethanol to this newly formed radical involves the detachment of a three protons (one from the hydroxyl termination of ethanol and two from its CH_2 group).

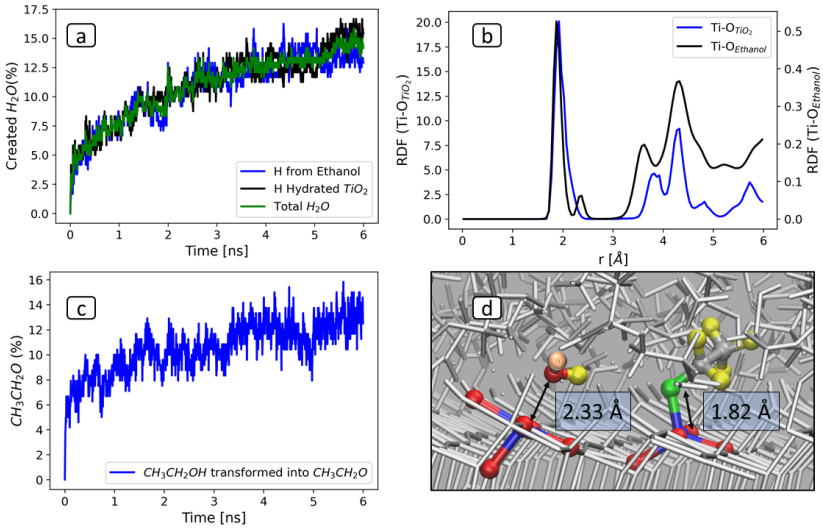

Figure 5: (a) Time evolution of the total number of H_2O, H from ethanol, and H from the initial hydration of TiO_2(101) incorporated into the water medium during the 1 ns, 400 K simulation. (b) Ti-O RDF distinguishing O from TiO_2(101) and O belonging to ethanol. (c) Number of newly adsorbed CH_3CH_2O radicals (ethyl alcohol molecules) *via* their oxygen onto the hydrated TiO_2(101) surface interface throughout the simulation. (d) Snapshot showing the local surface configuration immediately after ethanol dissociation, with the adsorption of the created water molecule and ethoxy radical bonding to titanium; O_{TiO_2} (red), Ti (blue), H_{TiO_2} (orange), $C_{Ethanol}$ (gray) atoms, $H_{Ethanol}$ (yellow) atoms, and $O_{Ethanol}$ (green) atoms. The number of oxygen atoms of the new CH_3CH_2O radicals binding to the hydrated TiO2 surface is calculated using a cutoff of Ti−O= 2.4 Å.

Furthermore, it is crucial to note that throughout the simulation, the C——C bonds in ethanol remains intact, indicating the absence of dissociation of ethanol into smaller organic carbon-based fragments, such as CO_2 or CH_4 for instance. The RDF curve shows that each carbon atom is coordinated by one atom at a distance of 1.58 Å. The dissociation of the C——C

bond is a problem encountered with some other photocatalysts. as an example, it was observed, after studying the dark catalytic reactions of ethanol over a series of catalysts based on CeO_2, that the bottleneck of the reaction lies in the breaking of the carbon-carbon bond of the ethanol molecules [47, 48].

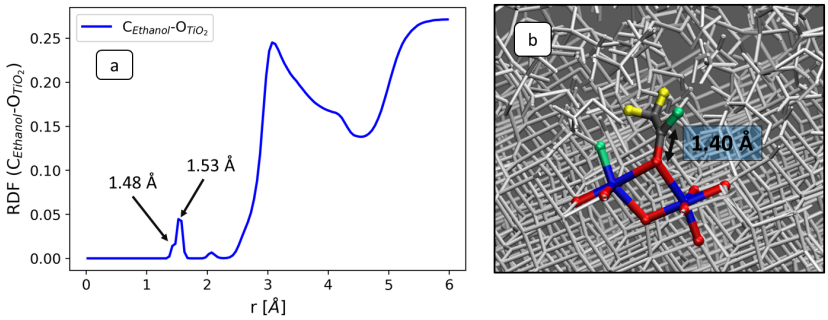

Figure 6: (a) Radial distribution function (RDF) between the carbon of ethanol and oxygen from the hydrated TiO_2(101) surface, illustrating (b) the formation of acetic acid radicals at the hydrated TiO_2(101) surface: O_{TiO_2} (red), Ti (blue), H_{TiO_2} (orange), $C_{Ethanol}$ (gray) atoms, $H_{Ethanol}$ (yellow) atoms, and $O_{Ethanol}$ (green) atoms.

3.1.3. Interactions at the water-ethanol mixture-TiO_2(101) Interface

We finally consider a mixed water-ethanol liquid phase (half/half in volume) in contact with TiO_2(101). Figure 7a illustrates the time-dependent formation of surface ethoxy radicals, which serves as a signature of ethanol reaction (see the corresponding configuration in Figure 7i). It is observed that, compared to pure liquid ethanol where roughly 14% coverage of ethoxy species is reached after 6 ns of annealing, and still increasing, the water-ethanol mixture exhibits a drop in radical formation down to only 2% coverage, which coverage rapidly saturates within the first ns. This indicates that the presence of water inhibits surface ethoxy formation. This can be attributed to the competitive adsorption of both molecules in favour of water, which will be quantified in the next subsection. In contrast to the few instances of CH_3O_2 formation observed at the ethanol-TiO_2(101) interface, this radical is not present in the case of the water-ethanol mixture.

Focusing on water reaction, the Figure 7b provides a quantification of oxygen exchange between water molecules and the substrate (configuration shown in Figure 7g). The proportion of oxygen atoms initially belonging to water molecules at the interface and binding to TiO_2(101) surface as hy-

droxyl groups amounts to approximately 20% coverage. In comparison, this quantity is decreased to 12% when water and ethanol are mixed, indicating that the presence of ethanol affects the surface binding behavior of water partly because of the permanent surface bonding of ethoxy radicals.

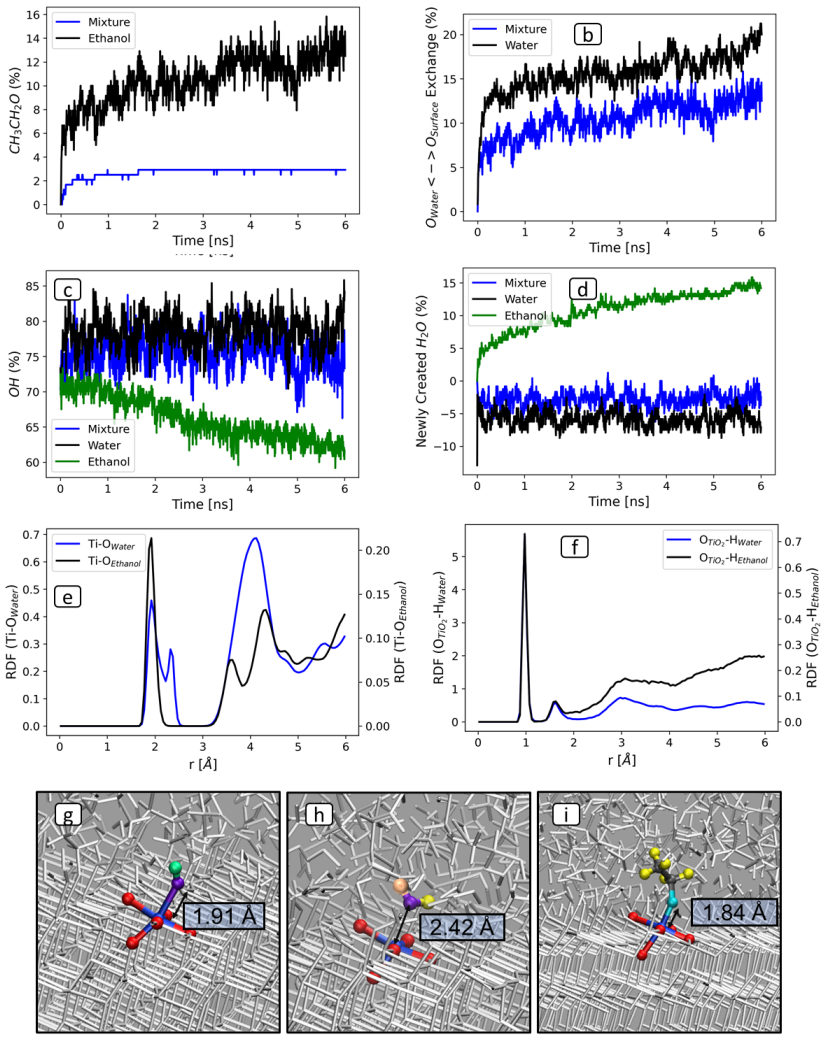

Figure 7: Comparison of water, ethanol, ethanol/water mixture interacting with hydrated TiO_2(101). Panels show: (a) temporal evolution of ethoxy coverage onto ceTiO2(101) exposed to ethanol and ethanol/water mixture , (b) temporal evolution of liquid to surface oxygen exchange in both water and ethanol/water mixture based systems, (c) temporal evolution of the total surface OH content in the three considered systems, (d) counts the quantity of water molecules being created/annihilated over time in the three considered systems. Panels (e,f) show the Radial Distribution Functions (RDFs) of Ti with respect to oxygen and hydrogen atoms from both water and ethanol, respectively. (g-i) depict snapshots of a selection of adsorbates onto TiO_2, respectively a OH that forms after water dissociation, an adsorbed water molecule being generated after ethanol dissociation, and an ethoxy radical

Figure 7e illustrates the radial distribution function (RDF) of surface Ti adsorption sites, distinguishing the bonding with oxygen initially belonging to water molecules with oxygen atoms, distinguishing their origin, i.e., water (blue curve) and ethanol (black curve). The latter exhibits a single peak at around 1.9 Å, suggesting a single form of bonding, corresponding to the ethoxy binding. Considering the RDF signature associated to oxygen from water, the resulting formation of OH gets a similar RDF signature (the Ti-O bond being approximately identical). But one additional peak is now present, at 2.4 Å), which is attributed to the non dissociative adsorption of water on surface Ti, at a distance of 2.4 Å(Figure 7h).

Notably, similarly to water and ethanol interfaces, the ethanol/water based system shows H-exchanges between the molecules and the hydrated surface. This exchange is clearly evidenced by the RDF signatures as shown in Figure 7f, where a peak at 0.98 Å is observed, assigned to surface oxygen atoms forming hydroxyls and H initially belonging to water molecules.

Comparing the three investigated interfaces in terms of the quantity of OH in Figure 7c, pure water and mixed ethanol/water cases show almost equivalent OH coverages, reaching approximately 78% and 72% coverage, respectively. Again, this indicates a dominance of water behaviour, while ethanol is responsible for the lowering of hydroxyl coverage. Note that the hydration level remains constant over the annealing. In contrast, in the case of pure ethanol, the quantity decreases gradually down to 64% coverage, as more and more ethoxy are being attached to the surface. Counting the number of water molecule as a function of time in Figure 7d shows that, while a pure ethanol exposure will lead to an increase of water molecules in the liquid phase (plus roughly 15 water molecules), water alone and the ethanol/water mixture cases experience a slight decrease in number, pointing again to the dominant role of water when competing with ethanol.

3.2. Mechanisms of Hydration and Molecular Hydrogen Production

The following subsection is dedicated to the energetics and pathways of hydration mechanisms, specifically on the interface capability to produce surface hydroxyl groups. These have been demonstrated to play an essential role in promoting hydrogen production during the photoreduction of water [41, 49], which chemical processes will be addressed next. From the previous sections, hydroxyl groups can be produced through the release of protons from the dissociation of both ethanol and water molecules. Potential pathways and associated energetic signatures of these mechanisms are

investigated using PMF calculations. All following pathways were evaluated at the ethanol/water-TiO_2(101) interface, at 300 K.

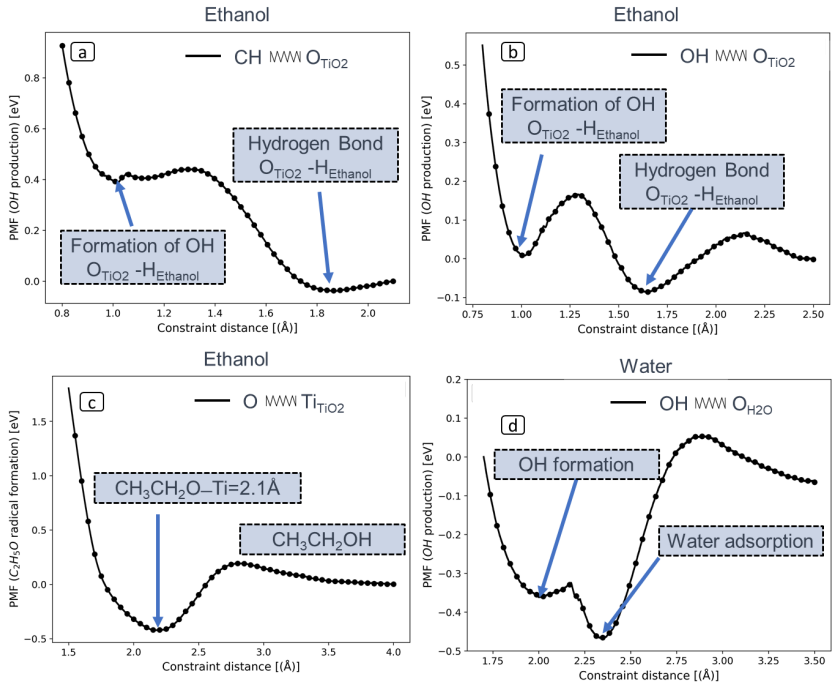

Figure 8: PMF energy profiles along reaction pathways for the generation of surface OH species through: (a) bonding of H from CH ethanol subunit onto a surface oxygen atom, (b) bonding of H of OH ethanol subunit onto a surface oxygen atom, (c) bonding of CH_3CH_2O onto a surface Ti atom, OH being created subsequently via the released H atom (d) bonding of H from H_2O onto a surface oxygen atom. Calculations were performed at the ethanol/water-TiO_2(101) interface at 300 K.

Figure 8a depicts the potential of mean force (PMF) energy curve along the reaction pathway relative to the formation of one specific OH hydroxyl at the TiO_2(101) surface, *via* a proton transfer from ethanol, initially located at its CH subunit. This process unfolds into two discernible stages. The initial stage involves the non dissociative adsorption of ethanol *via* a hydrogen bond formation, as $CH_3OH{-}HCH\cdots O_{TiO_2} = 1.8$ Å. Importantly, this stage does not necessitate overcoming any energy barrier. Transitioning to the second stage, the creation of a TiO——H bond requires an energy barrier of 0.45 eV, which falls into the room temperature class of mechanisms. Note that after dissociation, the under-coordinated carbon spontaneously react with a

neighboring H_2O to create an acetic acid molecule. In Figure 8b and c, we examine the surface OH formation from the release of the proton from the OH alcohol termination. Two paths are envisaged by directing the bond creation either between the hydrogen of the alcohol termination and a surface oxygen atom ($CH_3CH_2{-}OH\cdots O_{TiO_2}$, Figure 8b), or between the oxygen atom from the alcohol termination and a surface Ti atom ($CH_3CH_2{-}HO\cdots Ti_{TiO_2}$, Figure 8c). In the first case, a non dissociative adsorption of ethanol is established first via a hydrogen bond, $CH_3CH_2{-}OH\cdots O_{TiO_2}$ at a distance of 1.65Å, which shows an exothermic profile. Interestingly, while a more stable state is observed (roughly -0.1 eV) compared with the adsorption through the CH group, a small energy barrier is now to be overcome (O.O7 eV). While this barrier is not significant at room temperature, it might the reason for a configurational adaptation associated to a narrower pathway explaining the prevalence of the CH-based ethanol adsorption configuration observed in the simulations, for which no barrier is seen. Further decreasing the $OH_{\text{Ethanol}}\cdots O_{TiO_2}$ bond distance, ethanol dissociates with an energy barrier of 0.25 eV. The dissociation is slightly endothermic because of the strong collective stabilization (solvation) of the non dissociative adsorbate. In the second path, the formation of the ethoxy is realized first, leading to the release of a proton that in turn forms a surface hydroxyl. As pictured in Figure 8c, the pathway presents a exothermic profile, with an activation barrier of 0.2 eV and a better energy stabilization of -0.4 eV after dissociation. In a comparable vein, Density Functional Theory (DFT) was used to investigate the adsorption and dissociation of a single ethanol molecule on various surfaces of anatase [46]. The TiO_2(101) surface emerged as the most favorable substrate for the initial dissociation step of ethanol, leading to the creation of the CH_3CH_2O species. The calculated barrier activation energy for this step was established to be of 0.9 eV, at 0 K (with almost no gain in energy after dissociation). [46]

We now explore the formation of surface hydroxyl *via* water molecules. Two pathways are investigated depending on the water adsorption configuration, forming either a hydrogen bond through one of its H atom, or forming a dative bond via its O atom, with respectively their surface O and Ti atoms counterparts. The non dissociative adsorption of water via its hydrogen atoms and surface oxygen atom is unlikely as shown in Figure SM3, with an endothermic path and a positive energy for the adsorption state. In Figure 8d, the hydration through the direct formation of OH *via* after water dissociation onto surface Ti atom shows first a non dissociative adsorption

state which stabilizes at a distance of 2.34 Å with an energy of -0.4 eV (negligible activation barrier of 0.05 eV). Dissociation is calculated to be slightly endothermic, with a barrier of 0.13 eV, to form a Ti——OH group with a Ti-O bond length of 2.00 Å. The overall profile is similar to previous publication using *ab initio* deep potential molecular dynamics [1].

In summary, all calculated pathways are characterized by energy barriers below 0.5 eV making these events feasible at room temperature as well as observable in most of our molecular dynamics simulations. In this frame, PMF profiles allows interpreting their occurrence and statistics in terms of: the access to the adsorption sites, which is particularly true for ethanol dissociation through its OH termination; and the local arrangement of chemical species that is needed to stabilize the system during and after the biased reaction. In this latter case, dissociation of ethanol via its CH subunit appears unlikely, as for the adsorption of water through a $OH-H\cdots O_{TiO_2}$. Results indicate that water, more than ethanol can stick to the surface (better adsorption) while ethanol needs also to adapt its configuration due to steric hindrance. It is worth noting that the results obtained for the interaction of ethanol and water with the hydrated $TiO_2(101)$ surface differ from what would be obtained under vacuum (Figure SM4). Solvation generally lowers adsorption energies by further stabilizing adsorbates, which is a collective stabilization process varying from case to case as illustrated in our simulations. This is particularly illustrated in comparing the energies of the $O\cdots O_H$ hydrogen bond versus the O-H chemical bond in Figure 8b, in favour of the hydrogen type of bonding, which hierarchy is inverted in vacuum, where the chemical bond show superior binding energy, as expected (Figure SM4).

The PMF technique is particularly suitable to investigate rare events, i.e., necessitating extended or even unreachable duration of simulated experiments. The generation of hydrogen molecules from the hydrated surface, which is a crucial step of the photocatalysis process, is one such rare event that has not been observed across any of the analyzed interfaces. Our purpose is to investigate potential pathways either exclusively emanating from the surface, or being generated at the exact molecule-surface frontier. This latter type of mechanism is illustrated in Figure 9a and b, giving the PMF energy profiles of the selected reactions respectively under solvent exposure or in vacuum (a single molecule is then considered in contact to the surface). Three different mechanisms are investigated, with H_2 resulting from the recombination: (i) a H atom from a water molecule with a surface H atom (Figure 9a, blue curve), (ii) a H atom from the OH ethanol termination with

a surface H atom (Figure 9a, black curve), (iii) a H atom from the CH ethanol subunit with a surface H atom (Figure 9a, green curve). The analogous Figure 9b considers the same mechanisms, under vacuum. All energy profiles show high barrier in the range 4 to 5 eV, making hydrogen generation unlikely at reasonable temperature. However, simulation results indicate that the catalytic reaction either *via* the ethanol CH subunit or water (only when solvated) show lower activation (4.5 and 4.4 eV, respectively) compare to all other cases.

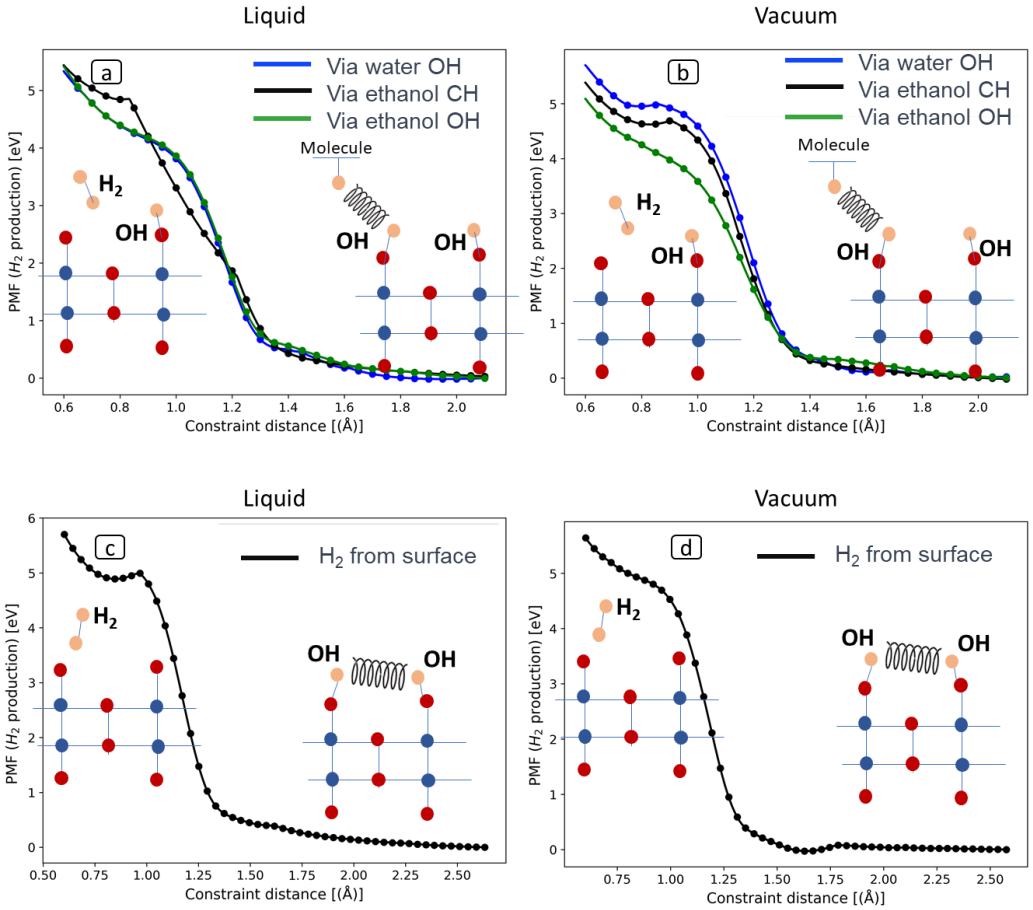

Figure 9: PMF energy profiles along reaction pathways for the generation of H_2: (a) via molecule/surface interaction under liquid exposure, (b) via single molecule/surface interaction under vacuum conditions, (c) through interacting surface hydroxyl species under solvent exposure, (d) similar case as (c), but under vacuum. These calculations were performed at 300 K, the liquid phase being composed of a mixture of ethanol and water.

It is now considered the generation of H_2 exclusively driven by surface mechanisms, through the hoping of surface H atoms belonging to hydroxyl species. The energy profile show similar trend as in the case of molecule/surface interactions but fail to produce barriers inferior to 5 eV range. Overall, these tentative mechanisms pleads for the prevalence of hydrogen generation through the molecule/surface complexes rather than being exclusively surface driven mechanisms. The relatively high value dispels

the likelihood of spontaneous H_2 formation across the considered interfaces, which is expected since optical or electrical excitation is required experimentally, at room temperature. One other potential perspective is to consider higher degree of chemical cooperativity at around reaction sites.

An alternative perspective on the surface's capacity to generate hydrogen is to assess its aptitude for transporting hydrogen species across its structure, a crucial step in orchestrating the configuration of catalytic species within a practical timeframe. This evaluation involves the computation of the Mean Square Displacement (MSD) in the time window of the last nanosecond of simulation. In our molecular dynamics (MD) simulations, we determine self-diffusion coefficients (D) utilizing Einstein's relation and a three-dimensional material model based on the mean square displacement (MSD). The MSD equation is defined as $\text{MSD} = \langle \delta r^2 \rangle = \frac{1}{N} \sum_i [r_i(t + t_0) - r_i(t_0)]^2$. Following the MSD computation, the self-diffusion coefficient (D) is ascertained as $D = \lim_{t\to\infty} \frac{\langle \delta r^2 \rangle}{6t} = \lim_{t\to\infty} \frac{\langle \text{MSD} \rangle}{6t}$[50, 51, 52]. These displacements are calculated at each iteration of the last nanosecond of the molecular dynamics simulations, where the steady state is reached with almost no chemical exchange between the liquid and solid phases. These MSD values are reported in Figure 10 for the three considered liquid phase e.g., water, ethanol and water/ethanol mixture. Results clearly show that ethanol inhibits surface migration of hydrogen. The calculated diffusion coefficient D are $8.45 \times 10^{-5}(\pm 1 \times 10^{-7})$ cm^2/s, $1.91 \times 10^{-5}(\pm 5 \times 10^{-8})$ cm^2/s, and $1.40 \times 10^{-7}(\pm 3 \times 10^{-9})$ cm^2/s for water, ethanol/water mixture, and ethanol-exposed hydrated surfaces, respectively. This confirms the major role of water, at the steady state of our simulations. Examination of the simulation trajectories indicate that Grotthuss mechanisms are driving the transport of hydrogen, which necessitates high OH coverage.

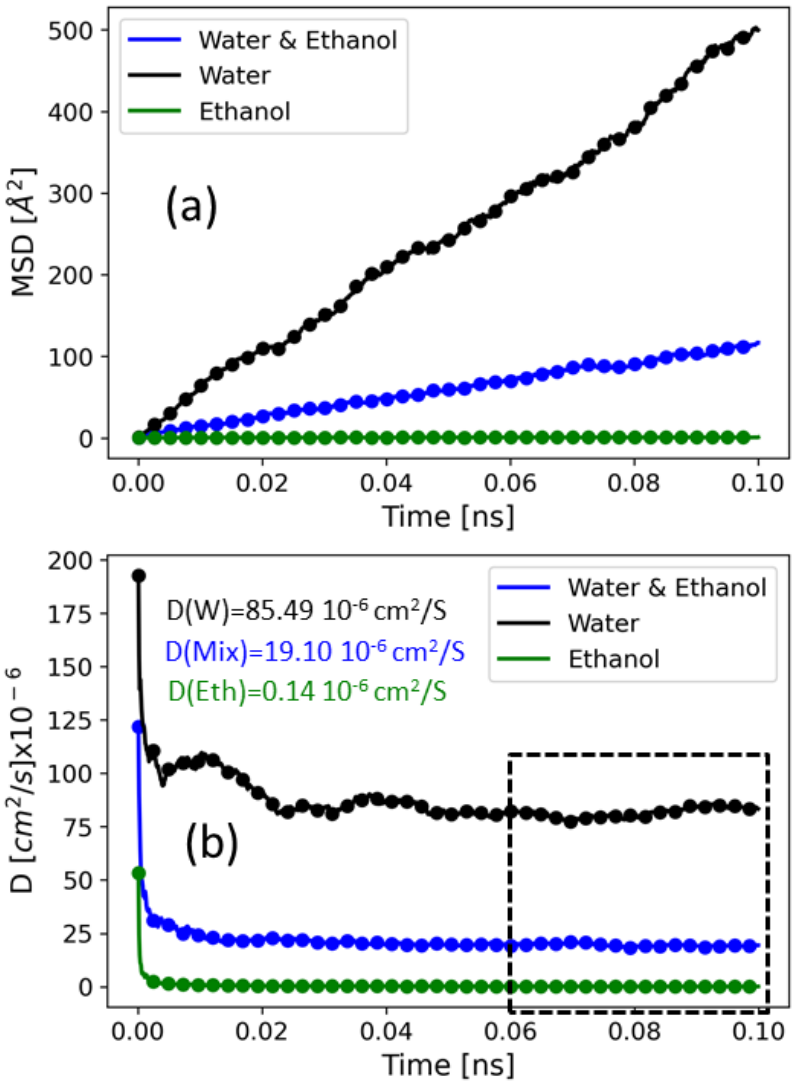

Figure 10: (a) Mean Square Displacement (MSD) and (b) Diffusion Coefficient (D) calculated over the last nanosecond of H formation in the hydration region of the TiO_2(101) surface, observed at three distinct surfaces: the mixture (water/ethanol)-hydrated TiO_2(101) surface, the water-hydrated TiO_2(101) surface, and the ethanol-hydrated TiO_2(101) surface.

4. CONCLUSION

In this study, we employed ReaxFF molecular dynamics simulations to delve deeper insights into the intricate dynamics of interactions involving

water, ethanol, their mixture onto hydrated TiO_2(101) surfaces. At the water-TiO_2(101) interface, surface hydrogen atoms catalyze the formation of hydroxyl groups, while surface hydrogen and oxygen atoms (to a lesser extent), exchange with the surrounding liquid phase. Moving to the ethanol-TiO_2(101) interface, the emergence of ethoxy radicals (CH_3CH_2O) species getting permanently bonded to surface Ti atoms, are shown to shadow the surface, slightly lowering hydroxyl surface density, but affecting much the hydrogen transport at the surface by three order of magnitude in their diffusion coefficient. More anecdotally, calculation reveals instances of CH_3CO_2 species adorning surface Ti sites *via* their oxygen atoms. The mixed water-ethanol-TiO_2(101) interface exhibits reduced ethoxy radicals and CH_3CO_2 suppression, which allows keeping a high ratio of hydroxyl groups, pointing also to the dominant and competing role of water when mixed to alcohol. PMF calculations offer insights into the underlying mechanisms of hydration. Both the dissociation of ethanol and water orchestrate the formation of hydroxyl groups on the TiO_2(101) surface through protonation, overcoming barriers below 0.45 eV. Notably, non-dissociative adsorption of these entities exhibits lower free energy than their dissociative counterparts due to efficient solvation of the non-dissociative adsorbates. Water shows the lowest adsorption energy, which is key to the water superior reactivity with the surface, tuning the overall surface interactions. Finally molecular hydrogen formation is discussed using the PMF technique, differentiating catalytic mechanisms, i.e., involving molecule (water or ethanol) surface interactions, from purely surfacic interactions (between adjacent surface hydroxyl groups). All calculated barrier are greater than 4 eV, making all tested mechanisms unlikely at reasonable temperature, which is expected since external excitations (optical, electrical) are known to be indispensable to achieve hydrogen recombination. Anyhow, our results suggest a prevalence (by 0.6 eV) of catalytic, versus purely surfacic mechanisms for generating molecular hydrogen.

5. Acknowledgement

The authors gratefully acknowledge the support received from the RHYO and Defi cle hydrogene vert from the Occitanie region. Additionally, we would like to express our appreciation for the generous provision of high−power computing resources by CALMIP for conducting this research.

6. Competing Interests

The authors declare that there are no conflicts of interest, encompassing both personal relationships and financial factors, which could have influenced the publication of the study presented in this article.

7. Supplementary Material

Here we present additional analyses, configuration snapshots, radial distribution functions (RDFs), and mean force potential (PMF) calculations to reinforce the conclusions advanced in the main content of this article.

References

[1] M. F. C. Andrade, H.-Y. Ko, L. Zhang, R. Car, A. Selloni, Free energy of proton transfer at the water–tio 2 interface from ab initio deep potential molecular dynamics, Chemical Science 11 (9) (2020) 2335–2341.

[2] K. A. Oyekan, M. Van de Put, S. Tiwari, C. Rossi, A. Esteve, W. Vandenberghe, Re-examining the role of subsurface oxygen vacancies in the dissociation of h2o molecules on anatase tio2, Applied Surface Science 594 (2022) 153452.

[3] M. I. Mendoza Diaz, A. Balocchi, K. Oyekan, K. Tan, W. G. Vandenberghe, A. Esteve, C. Rossi, Dominant role of oh- and ti3+ defects on the electronic structure of tio2 thin films for water splitting, Dalton Trans. 51 (2022) 15300–15311.

[4] G. Fisicaro, S. Filice, S. Scalese, G. Compagnini, R. Reitano, L. Genovese, S. Goedecker, I. Deretzis, A. La Magna, Wet environment effects for ethanol and water adsorption on anatase tio2 (101) surfaces, The Journal of Physical Chemistry C 124 (4) (2019) 2406–2419.

[5] J. A. Khan, M. Sayed, N. S. Shah, S. Khan, Y. Zhang, G. Boczkaj, H. M. Khan, D. D. Dionysiou, Synthesis of eosin modified tio2 film with co-exposed {001} and {101} facets for photocatalytic degradation of para-aminobenzoic acid and solar h2 production, Applied Catalysis B: Environmental 265 (2020) 118557.

[6] J. O. Hansen, P. Huo, U. Martinez, E. Lira, Y. Y. Wei, R. Streber, E. Lægsgaard, B. Hammer, S. Wendt, F. Besenbacher, Direct evidence for ethanol dissociation on rutile tio_2(110), Phys. Rev. Lett. 107 (2011) 136102.

[7] M. Raju, S.-Y. Kim, A. C. Van Duin, K. A. Fichthorn, Reaxff reactive force field study of the dissociation of water on titania surfaces, The Journal of Physical Chemistry C 117 (20) (2013) 10558–10572.

[8] Z. Futera, N. J. English, Exploring rutile (110) and anatase (101) tio2 water interfaces by reactive force-field simulations, The Journal of Physical Chemistry C 121 (12) (2017) 6701–6711.

[9] A. Fujishima, K. Honda, Electrochemical photolysis of water at a semiconductor electrode, Nature 238 (1972) 37–38.

[10] X. Zhang, S. Zhang, X. Cui, W. Zhou, W. Cao, D. Cheng, Y. Sun, Recent advances in tio2-based photoanodes for photoelectrochemical water splitting, Chemistry–An Asian Journal 17 (20) (2022) e202200668.

[11] P. Deak, J. Kullgren, B. Aradi, T. Frauenheim, L. Kavan, Water splitting and the band edge positions of tio2, Electrochimica Acta 199 (2016) 27–34.

[12] R. Marschall, Semiconductor composites: strategies for enhancing charge carrier separation to improve photocatalytic activity, Advanced Functional Materials 24 (17) (2014) 2421–2440.

[13] L. Huang, K. E. Gubbins, L. Li, X. Lu, Water on titanium dioxide surface: a revisiting by reactive molecular dynamics simulations, Langmuir 30 (49) (2014) 14832–14840.

[14] J. Rey, P. Clabaut, R. Réocreux, S. N. Steinmann, C. Michel, Mechanistic investigation and free energies of the reactive adsorption of ethanol at the alumina/water interface, The Journal of Physical Chemistry C 126 (17) (2022) 7446–7455.

[15] J. J. Karnes, E. A. Gobrogge, R. A. Walker, I. Benjamin, Unusual structure and dynamics at silica/methanol and silica/ethanol interfaces a molecular dynamics and nonlinear optical study, The Journal of Physical Chemistry B 120 (8) (2016) 1569–1578.

[16] G. Nakhate, V. Nikam, K. Kanade, S. Arbuj, B. Kale, J. Baeg, Hydrothermally derived nanosized ni-doped tio2: a visible light driven photocatalyst for methylene blue degradation, Materials Chemistry and Physics 124 (2-3) (2010) 976–981.

[17] Z. Dong, D. Ding, T. Li, C. Ning, Ni-doped tio2 nanotubes photoanode for enhanced photoelectrochemical water splitting, Applied Surface Science 443 (2018) 321–328.

[18] C. Y. Toe, C. Tsounis, J. Zhang, H. Masood, D. Gunawan, J. Scott, R. Amal, Advancing photoreforming of organics: Highlights on photocatalyst and system designs for selective oxidation reactions, Energy & Environmental Science 14 (3) (2021) 1140–1175.

[19] A. V. Puga, Photocatalytic production of hydrogen from biomass-derived feedstocks, Coordination Chemistry Reviews 315 (2016) 1–66.

[20] H. Jabraoui, S. Gin, T. Charpentier, R. Pollet, J.-M. Delaye, Leaching and reactivity at the sodium aluminosilicate glass–water interface: Insights from a reaxff molecular dynamics study, The Journal of Physical Chemistry C 125 (49) (2021) 27170–27184.

[21] S.-Y. Kim, A. C. Van Duin, J. D. Kubicki, Molecular dynamics simulations of the interactions between tio2 nanoparticles and water with na+ and cl-, methanol, and formic acid using a reactive force field, Journal of Materials Research 28 (3) (2013) 513–520.

[22] S. Plimpton, Fast parallel algorithms for short-range molecular dynamics, Journal of computational physics 117 (1) (1995) 1–19.

[23] S.-Y. Kim, A. C. van Duin, Simulation of titanium metal/titanium dioxide etching with chlorine and hydrogen chloride gases using the reaxff reactive force field, The Journal of Physical Chemistry A 117 (27) (2013) 5655–5663.

[24] T. Al-Dhahir, Quantitative phase analysis for titanium dioxide from x-ray powder diffraction data using the rietveld method, Diyala journal for pure sciences 2 (9) (2013) 108–119.

[25] M.-I. Mendoza-Diaz, A. Lecestre, L. Salvagnac, B. Bounor, D. Pech, M. Djafari-Rouhani, A. Estève, C. Rossi, High surface area tio2 photocatalyst for h2 production through silicon micromachining, Applied Surface Science 588 (2022) 152919.

[26] H. Jabraoui, T. Charpentier, S. Gin, J.-M. Delaye, R. Pollet, Behaviors of sodium and calcium ions at the borosilicate glass–water interface: Gaining new insights through an ab initio molecular dynamics study, The Journal of Chemical Physics 156 (13) (2022).

[27] H. Jabraoui, T. Charpentier, S. Gin, J.-M. Delaye, R. Pollet, Atomic insights into the events governing the borosilicate glass–water interface, The Journal of Physical Chemistry C 125 (14) (2021) 7919–7931.

[28] A. J. Marsden, M. Skilbeck, M. Healey, H. R. Thomas, M. Walker, R. S. Edwards, N. A. Garcia, F. Vuković, H. Jabraoui, T. R. Walsh, et al., From graphene to graphene oxide: the importance of extended topological defects, Physical Chemistry Chemical Physics 24 (4) (2022) 2318–2331.

[29] R. Pollet, C. S. Bonnet, P. Retailleau, P. Durand, Tóth, Proton exchange in a paramagnetic chemical exchange saturation transfer agent from experimental studies and ab initio metadynamics simulation, Inorganic Chemistry 56 (8) (2017) 4317–4323.

[30] K. Damodaran, J.-M. Delaye, A. G. Kalinichev, S. Gin, Deciphering the non-linear impact of al on chemical durability of silicate glass, Acta Materialia 225 (2022) 117478.

[31] S. Izrailev, S. Stepaniants, B. Isralewitz, D. Kosztin, H. Lu, F. Molnar, W. Wriggers, K. Schulten, Computational molecular dynamics: Challenges, methods, in: Ideas, Vol. 4, 1998, p. 39.

[32] H. Jabraoui, M. D. Rouhani, C. Rossi, A. Esteve, First-principles investigation of cuo decomposition and its transformation into cu 2 o, Physical Review Materials 6 (9) (2022) 096001.

[33] S. Park, K. Schulten, Calculating potentials of mean force from steered molecular dynamics simulations, The Journal of chemical physics 120 (13) (2004) 5946–5961.

[34] C. Jarzynski, Nonequilibrium equality for free energy differences, Physical Review Letters 78 (14) (1997) 2690.

[35] H. Jabraoui, A. Alpuche, C. Rossi, A. Esteve, New insights into the mechanisms of tib2 (001) thermal oxidation combining molecular dynamics and density functional theory calculations, Acta Materialia 262 (2024) 119463.

[36] A. Benbella, H. Jabraoui, I. Matrane, M. Mazroui, Exploring adsorption behavior of sulfur and nitrogen compounds on transition metal-doped cu (100) surfaces: insights from dft and md simulations, Physical Chemistry Chemical Physics 25 (40) (2023) 27553–27565.

[37] H. Jabraoui, I. Khalil, S. Lebègue, M. Badawi, Ab initio screening of cation-exchanged zeolites for biofuel purification, Molecular Systems Design & Engineering 4 (4) (2019) 882–892.

[38] P. Losch, H. R. Joshi, O. Vozniuk, A. Grunert, C. Ochoa-Hernandez, H. Jabraoui, M. Badawi, W. Schmidt, Proton mobility, intrinsic acid strength, and acid site location in zeolites revealed by varying temperature infrared spectroscopy and density functional theory studies, Journal of the American Chemical Society 140 (50) (2018) 17790–17799.

[39] I. Khalil, H. Jabraoui, G. Maurin, S. Lebègue, M. Badawi, K. Thomas, F. Mauge, Selective capture of phenol from biofuel using protonated faujasite zeolites with different si/al ratios, The Journal of Physical Chemistry C 122 (46) (2018) 26419–26429.

[40] A. Tilocca, A. Selloni, Dft-gga and dft+ u simulations of thin water layers on reduced tio2 anatase, The Journal of Physical Chemistry C 116 (16) (2012) 9114–9121.

[41] M. I. Mendoza Diaz, A. Balocchi, K. Oyekan, K. Tan, W. G. Vandenberghe, A. Esteve, C. Rossi, Dominant role of oh- and ti3+ defects on the electronic structure of tio2 thin films for water splitting, Dalton Trans. 51 (2022) 15300–15311.

[42] B. Li, S. Wu, X. Gao, Theoretical calculation of a tio2-based photocatalyst in the field of water splitting: A review, Nanotechnology Reviews 9 (1) (2020) 1080–1103.

[43] K. Katsiev, G. Harrison, H. Alghamdi, Y. Alsalik, A. Wilson, G. Thornton, H. Idriss, Mechanism of ethanol photooxidation on single-crystal anatase tio2 (101), The Journal of Physical Chemistry C 121 (5) (2017) 2940–2950.

[44] H. Alghamdi, H. Idriss, Study of the modes of adsorption and electronic structure of hydrogen peroxide and ethanol over tio2 rutile (110) surface within the context of water splitting, Surface Science 669 (2018) 103–113.

[45] G. Mattioli, F. Filippone, R. Caminiti, A. Amore Bonapasta, Short hydrogen bonds at the water/tio2 (anatase) interface, The Journal of Physical Chemistry C 112 (35) (2008) 13579–13586.

[46] R. Zhang, Z. Liu, L. Ling, B. Wang, The effect of anatase tio2 surface structure on the behavior of ethanol adsorption and its initial dissociation step: A dft study, Applied Surface Science 353 (2015) 150–157.

[47] P.-Y. Sheng, G. Bowmaker, H. Idriss, The reactions of ethanol over au/ceo2, Applied Catalysis A: General 261 (2) (2004) 171–181.

[48] P.-Y. Sheng, A. Yee, G. Bowmaker, H. Idriss, H2 production from ethanol over rh–pt/ceo2 catalysts: the role of rh for the efficient dissociation of the carbon–carbon bond, Journal of Catalysis 208 (2) (2002) 393–403.

[49] M.-I. Mendoza-Diaz, J. Cure, M. D. Rouhani, K. Tan, S.-G. Patnaik, D. Pech, M. Quevedo-Lopez, T. Hungria, C. Rossi, A. Estève, On the uv–visible light synergetic mechanisms in au/tio2 hybrid model nanostructures achieving photoreduction of water, The Journal of Physical Chemistry C 124 (46) (2020) 25421–25430.

[50] H. Jabraoui, A. Esteve, M. Schoenitz, E. L. Dreizin, C. Rossi, Atomic scale insights into the first reaction stages prior to al/cuo nanothermite ignition: influence of porosity, ACS applied materials & interfaces 14 (25) (2022) 29451–29461.

[51] S. H. Hahn, A. C. van Duin, Surface reactivity and leaching of a sodium silicate glass under an aqueous environment: a reaxff molecular dynamics study, The Journal of Physical Chemistry C 123 (25) (2019) 15606–15617.

[52] H. Jabraoui, A. Estève, S. Hong, C. Rossi, Initial stage of titanium oxidation in ti/cuo thermites: a molecular dynamics study using reaxff forcefields, Physical Chemistry Chemical Physics 25 (16) (2023) 11268–11277.